International Journal of Development Mathematics Vol 1 Issue 2, Page No. 098 - 113

INTERNATIONAL JOURNAL OF DEVELOPMENT MATHEMATICS

ISSN: 3026-8656 (Print) | 3026-8699 (Online)

journal homepage: https://ijdm.org.ng/index.php/Journals

Significance of Viscous Dissipation on Hydromagnetic Oscillatory Flow Affected by Nanoparticles Through a Boundary Layer Regime

Emmanuel Omokhuale[a*], Godwin Ojemeri[b], Aminu Muhammad[a] and Halima Usman[c]

[a]*Department of Mathematics, Faculty of Sciences, Federal University Gusau, P. M. B. 1001, Zamfara State.*

[b]*Department of Mathematics, College of Sciences, Federal University of Agriculture, P. M. B. 28, Zuru, Kebbi State.*

[c]*Department of Mathematics, Faculty of Physical and Computing Sciences, Usmanu Danfodiyo University, P.M.B. 2346, Sokoto State, Nigeria*

ARTICLE INFO

Article history:
Received 08 March 2024
Received in revised form 08 April 2024
Accepted 19 May 2024

Keywords:
Chemical reaction, Magnetohydrodynamics (MHD), Nanofluid, Oscillatory flow, Viscous dissipation

MSC 2020 Subject classification:
34A25, 34B15, 34L05

ABSTRACT

In this article, the implications of viscous dissipation on buoyancy-induced heat and mass transfer of a nanofluid flow along a semi-infinite flat plate in an oscillating system is performed, taking into account the impacts of magnetohydrodynamics (MHD), chemical reaction, porous medium and heat sink. The consequences of various flow parameters on the velocity, temperature, and concentration distribution of the nanofluid, as well as the skin friction coefficient, Nusselt number, and Sherwood number has been solved semi-analytically. The basic governing equations have been determined by employing appropriate transformations techniques which result in high nonlinear coupled differential equations with physical conditions. Different types of nanoparticles are considered, and the salient features of all the embedded parameters on velocities, temperature and concentration fields have been displayed graphically and illustrated. It is concluded from the computational analysis that application of viscous dissipative parameter improves the temperature distributions, which consequently speed up the fluid velocity. This model has practical applications in the fields of biomedicine and resonance imaging. In addition, graphical comparison between Narayana and Venkateswarlu (2016) with the present work demonstrate an excellent relationship, thereby authenticating the precision and accuracy of this present work.

1. Introduction

Current advancements in nanotechnology have made it much easier to create nanoparticles or nanostructures with higher thermophysical properties than their bulk counterparts utilizing nuclear or molecular processes. Salah *et al.* (2023) developed Nano fluids by dispersing nanoparticles in a base fluid such as water, oil, or ethylene glycol, to name a few. The study of Nano fluids has witnesses a rise in research activities over the years. Choi (1995) introduced the first nan fluid theory. Several researchers have studied heat and mass transport in MHD Nano fluid flows. To this end, Usman and Sanusi (2023) recently explored the effects of non-Newtonian Nano fluid flows across a semi-infinite flat plate immersed in a porous medium on heat radiation, Soret, and pressure terms. They took into account the surface temperature and concentration, which are oscillatory in nature due to the presence of various types of nanoparticles. Salleh *et al.* (2010) investigated mixed convection boundary layer flow over a horizontal circular cylinder with Newtonian heating and found that heat transfer from the surface is proportional to the local surface temperature. Gbadeyan *et al.* (2020) studied the effect of changing thermal conductivity and viscosity on non-Newtonian Nano fluid flow when convective heating and velocity slip were present. Mehryan *et al.* (2016) examined the fluid flow and heat transfer analysis of a Nano fluid containing motile gyro tactic microorganisms passing a non-linear stretching vertical sheet in the presence of a non-uniform magnetic field; numerical approach and concluded that the density number of the motile microorganisms increases as the magnetic field, Grashof number, and Reynold number increase.

Satya *et al.* (2016) studied heat and mass transfer on MHD nanofluid flow past vertical porous plate in a

* Corresponding author. Tel.: +2348032878725
E-mail address: emmanuelomokhuale@gmail.com (Emmanuel O.).
https://doi.org/10.62054/ijdm/0102.07

rotating system effect, taking into account the influence of chemical reaction and heat source on MHD and eventually determining that the Copper nanoparticles proved to have the maximum cooling recital compared to Alumina and Titanium oxide. Prasad *et al.* (2018) conducted a rigorous examination of the heat and mass transfer analysis for the MHD flow of nanofluid with radiation absorptions. They investigated the effects of diffusion, thermodynamics, and chemical reactions on the free convection heat and mass transfer flow of nanofluid over a vertical plate embedded in a porous medium in the presence of radiation absorption and a heat source under fluctuating boundary conditions. The authors discovered that increasing the Dufour number and radiation absorption parameter leads to an increase in thermal boundary layer thickness, while decreasing the species concentration with increasing valence.

Baoku and Fadare (2018) investigated thermos-diffusion and diffusion-thermo effects on mixed convection hydromagnetic flow in a third-grade fluid over a stretching surface in a Darcy forchheimer porous medium and discovered that Soret and Dufour numbers increase as a function of species concentration and thermal boundary thickness. Mabood and Usman (2019) investigated the influence of numerous slips on MHD nanofluid boundary layer flow with heat and mass transfer in a Darcy porous media. They investigated the effect of Darcy number and magnetic field parameters in their work and discovered that increasing the Darcy number and magnetic field parameter leads to increased friction and heat transfer rate. Recently, Saleem *et al.* (2024) research on significance of hafnium nanoparticles in hydromagnetic non-Newtonian fluid-particle suspension model through divergent channel with uniform heat source.

Khedher *et al.* (2024) provided novel current research to control thermal and magnetic boundary layer in the presence of viscous dissipation and induced electromagnetic field.

The numerical analysis of convection movement of an oscillatory flow involving heat and mass transfer filled with porous medium through various flow channels have been performed by many authors. In this regard, Hamza *et al*. (2011) analyzed the impacts of chemical reaction and slip condition on a time-dependent hydromagnetic heat and mass transfer flow across an upstanding channel saturated with porous medium in a rotating system. Bafakeeh *et al*. (2022) discussed the unsteady hydromagnetic oscillatory natural convective heat and mass transfer flow of a viscous and electrically conducting fluid passing through a vertical plate immersed in a permeable medium in the coexistence of chemical reactions and thermal radiation affected by Hall current and Soret factor. Narayana and Venkateswarlu (2016) studied the consequences of chemical reaction and heat source effects on unsteady MHD free convection heat and mass transfer of a nanofluid flow past a semi-infinite flat plate in a rotating system. The plate is assumed to oscillate in time with steady frequency so that the solutions of the boundary layer are the similar oscillatory type.

Ramaiah *et al.* (2016) deliberated on the impacts of chemical reaction and radiation absorption on hydromagnetic natural convective heat and mass transfer flow of electrically-conducting visco-elastic fluid along permeable medium confined to an oscillating porous wall in the involvement of heat source and sink. Sharma *et al.* (2022) emphasized the analytical study of MHD oscillatory time-dependent free convective viscous incompressible dissipative flow passing through an upstanding channel entrenched with porous medium in the coexistence of heat generation and thermal radiation factors. Choudhury and Hazarika (2012) echoed the significance of variable viscosity and thermal conductivity on free convective oscillatory flow of a viscous incompressible and electrically conducting fluid past a vertical plate in slip flow regime with periodic plate temperature when suction velocity oscillates in time about a constant mean. Falade *et al.* (2017) investigated the implications of suction/injection effects on a time-dependent oscillatory slip flow within an upright vertical channel with unequal wall heating restricted to a transverse magnetic field.

Because it has so many applications in the chemical and hydrometallurgical industries, the study of heat and mass transfer flow in the presence of chemical reactions has attracted a lot of attention throughout the years. The two most prevalent types of chemical reactions are heterogeneous and homogeneous ones. A chemical reaction is called heterogeneous rather than homogeneous if it occurs at an interface as opposed to in a single phase throughout its volume. In contrast to a homogeneous reaction, which occurs evenly across the entire given phase, a heterogeneous reaction occurs in a confined area or inside the border of a phase. Melting, ceramics and glassware production, catalytic chemical reactors, polymer production, ceramics and glassware production, and the initiation of exothermic or endothermic chemical reactions are just a few of the numerous important applications of heat and mass transfer flows with chemical reactions (Bafakeeh *et al.* 2022). A number of investigators, conscious of the significance of this type of research, have investigated the hydromagnetic free convection heat and mass transfer flow of a viscous, incompressible, and electrically conducting fluid moving through an upright plate in the presence of a chemical reaction influenced by a variety of flow circumstances. A number of scientists investigated the effect of chemical reactions on various fluid flow regimes. Raghunath *et al.* (2022) explored MHD Casson fluid flow across a vertical porous plate under the influence of heat diffusion and chemical reaction in this context. The impact of a chemical reaction on the erratic hydromagnetic natural convective coquette flow in a vertical channel packed with porous materials was studied by Ajibade *et al.* (2016). Other studies that looked at how different flow geometries are affected by chemical interactions are included below. To name a few, Muthucumaraswamy (2002), Raghunath *et al.* (2021), Raghunath and Obulesu (2022), Reddy *et al.* (2022), Ibrahim *et al.* (2008), and Kesavaiah *et al.* (2011).

A porous medium, according to Mahmoudi *et al.* (2020), is a solid matrix with void spaces called pores that are linked by a system of channels through which fluid can flow. So many scientists' attention has been drawn to convection in porous media because of its more engineering applications to areas such as geothermal systems, solid matrix heat exchangers, thermal insulations, oil extraction and store of nuclear waste materials and so forth. This phenomenon can also be used for underground coal gasification, ground water hydrology, wall cooled catalytic reactors, cooling of nuclear reactors, solar power collectors and energy efficient drying processes. Several researches have been conducted to demonstrate the significance of both free and mixed convection flows equipped with porous medium through various flow channels under different physical settings. To this end, Ajibade *et al.* (2023) recently investigated the effects viscous and Darcy dissipation in a steady fully developed free convection flow in a composite channel partially saturated with porous medium due heat generation using homotopy perturbation approach.

Natural convection in porous media in a highly nonlinear metaphysical engineering applications was demonstrated by Kadeethum *et al.* (2022). The MHD convection flow of Casson fluid in micro-channels including porous material was discussed by Gireesha and Sindhu (2020). When Alam *et al*. (2021) used network simulation method solutions to analyze time-dependent hydro-magnetic radiative fluid flow over an inclined porous plate with heat and mass permeability, they found that the fluid momentum tended to rise or fall gradually towards the plate and then diminish or grow slowly away from the plate. The temperature of the fluid has been reported to exhibit the same tendency. Abbas *et al.* (2022) examined various industrial operations involve frequent heating and cooling of electrical systems through porous medium. Alvarez *et al.* (2022) study a stationary double diffusive natural convection problem in porous medium. Khalil *et al*. (2022) explored heat transfer by natural convection within the trapezoidal enclosure. Hamza *et al*. (2022) analysed a time-dependent hydromagnetic buoyancy-induced flow of a chemically reactive fluid in a convectively heated upstanding channel coated with porous material affected by Newtonian heating conditions. It was concluded that the fluid velocity experiences a surge as the porous medium, thermal Biot number, slip parameter and the viscous reactive fluid parameter increased. Bordoloi *et al.* (2021) deliberated on the Dufour effect on three-dimensional flow along a porous vertical plate in a porous medium with periodic suction and permeability. Later, Bordoloi *et al.* (2023) outlined an analytical solution for two-dimensional steady, viscous, incompressible hydromagnetic free convective flow across a uniformly stretching upstanding porous plate submerged in a porous medium in the coexistence of Soret effect and chemical reaction.

The ultimate aim of this research is to extend the work of Narayana and Venkateswarlu (2016) by investigating the influence of viscous dissipative fluid on a thermally and chemically controlled MHD oscillatory flow affected by nanoparticles in the involvement of chemical reaction and porous material through a porous upstanding channel. The resultant highly nonlinear partial differential equations in terms of temperature, concentration and velocity are solved by regular perturbation method. various illustrative graphs have been plotted under the influence of some nanoparticles to showcase the flow pattern of the pertinent embedded parameters dictating the flow. Internal heating is a type of mechanical energy dissipation that is spurred on by viscous forces in molecular fluid-particle exchanges. This particular kind of mechanical energy dissipation has a major effect on the fluid's hydrodynamic and thermodynamic behavior, and its attributes have a wide range of applications in the lubrication, food processing, and food preservation industries, as well as in the cooling of electrical appliances, exploration for petroleum products, and other industries. Further, in physics, chemistry, and engineering, the combination of key characteristics such as nanoparticles and heat generating systems has been very effective in improving the thermal conductivity of the base fluid and solar collection system.

2. Mathematical Formulation of the Flow Problem

Imagine an unsteady MHD nanofluid flow past a semi-infinite vertical permeable plate in a rotating system with chemical reaction, thermal diffusion and thermal radiation in the presence of a uniform transverse magnetic field. It is assumed that there is no applied voltage which implies the absence of an electric field. The flow is assumed to be in the x -direction which is taken along the plate in the upward direction, the Y –axis is normal to it and the z axis along the width of the plate as shown in Figure 1. Also it is assumed that the whole system is rotate with a constant vector Ω about z –axis. Due to semi-infinite plate surface assumption the flow variables are functions of z and time t only. Following Narayana and Venkateswarlu (2016) and assuming that the fluid is controlled by viscous dissipation effect, the governing equations of this model can be written in dimensional form as follow:

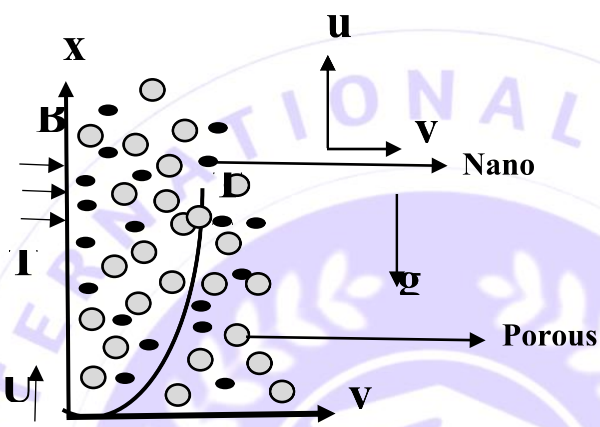

Figure 1: Physical Configuration of the flow system

Continuity Equation:

$$\frac{\partial w'}{\partial z'} = 0 \tag{1}$$

Momentum Equation:

$$\frac{\partial u'}{\partial t'} + w'\frac{\partial u'}{\partial z'} - 2\Omega = \frac{1}{\rho_{nf}}\left\{\mu_{nf}\frac{\partial^2 u'}{\partial z'^2} + (\rho\beta)_{nf}g\beta(T' - T'_\infty) - \frac{v_f u'}{k} - \frac{\sigma\beta_0^2 u'}{\rho}\right\} \tag{2}$$

$$\frac{\partial v'}{\partial t'} + w'\frac{\partial v'}{\partial z'} + 2\Omega u' = \frac{1}{\rho_{nf}}\left\{\mu_{nf}\frac{\partial^2 v'}{\partial z'^2} - \frac{v_f v'}{k} - \frac{\sigma\beta_0^2 v'}{\rho}\right\} \tag{3}$$

Energy Equation:

$$\frac{\partial T'}{\partial t'} + w'\frac{\partial T'}{\partial z'} = \alpha_{nf}\frac{\partial^2 T'}{\partial y'^2} - \frac{Q_H}{(\rho C_P)_{nf}}(T' - T'_\infty) + \frac{v}{c_\rho}\left[\left(\frac{\partial U'}{\partial z'}\right)^2\right] \tag{4}$$

Mass Concentration /Diffusion Equation:

$$\frac{\partial c'}{\partial t'} + w'\frac{\partial c'}{\partial z'} = D_m\frac{\partial^2 c'}{\partial z'^2} + D_L\frac{\partial^2 T'}{\partial z'^2} - R_m(C' - C'_\infty) \tag{5}$$

The appropriate boundary conditions are:

$$u'(z't') = 0, v'(z't') = 0, T(z't') = 0,\ C(z't') = 0\ \ for\ t' \le 0$$
$$u'(z't') = 1 + \frac{\varepsilon}{2}(e^{int} + e^{-int}), v(0,t) = 0, T(0,t') = 1,\ C(0,t') = 1$$
$$u'(\infty,t') \to 0, v'(\infty,t') \to 0, T'(\infty,t') \to 0,\ C'(z't') \to 0\ for\ t \ge\ 0 \tag{6}$$

The properties of nanofluids are defined as follows:

$$p_{nf} = (1-\emptyset)p_f + \emptyset p_s,\ (\rho C_p)_{nf} = (1-\emptyset)\quad (\rho C_p)_f + \emptyset(\rho C_p)_s$$
$$(\rho\beta)_{nf} = (1-\emptyset)\quad (\rho\beta)_f + \emptyset(\rho\beta)_s,\ \mu_{nf} = \frac{\mu_f}{(1-\emptyset)^{2.5}},\ \alpha_{nf} = \frac{K_{nf}}{(\rho C_p)_{nf}}$$
$$K_{nf} = K_f\left\{\frac{K_s + 2K_f - 2\emptyset(K_f - K_s)}{K_s + 2K_f + 2\emptyset(K_f - K_s)}\right\} \tag{7}$$

Introducing the following nondimensional quantities are:

$$u = \frac{u'}{U_0}, v = \frac{v'}{U_0}, z = \frac{U}{vf}z', t = \left(\frac{vf}{U^2}\right)t', n = \left(\frac{U^2}{vf}\right)n', R = \frac{2\Omega vf}{U^2}, S = \frac{w_0}{U}, Sc = \frac{v}{D_B}, Sr = \frac{D_T(T_w - T_\infty)}{(C_w - C_\infty)T_\infty}\ \ , T =$$

$\frac{(T-T_\infty)}{(T_w-T_\infty)}, C = \frac{(C-C_\infty)}{(C_w-C_\infty)}, B_r = EcPr$ where $Ec = \frac{U_0^2}{c_p\left(T_w - T_\infty\right)}$ and $\Pr = \frac{\nu}{\alpha_{nf}}$ (8)

Inserting eqn (8) into eqns (2-6), we have the following dimensionless equations:

$$A_3\left\{\frac{\partial u}{\partial t} - S\frac{\partial u}{\partial z} - Rv\right\} = \frac{1}{A_1}\frac{\partial^2 u}{\partial z^2} + A_4 T - \left(M + \frac{1}{K}\right)u \tag{9}$$

$$A_3\left\{\frac{\partial u}{\partial t} - S\frac{\partial u}{\partial z} - Ru\right\} = \frac{1}{A_1}\frac{\partial^2 u}{\partial z^2} - \left(M + \frac{1}{K}\right)v \tag{10}$$

$$A_5\left\{\frac{\partial T}{\partial t} - S\frac{\partial T}{\partial z}\right\} = \frac{1}{Pr}\left\{A_2\frac{\partial^2 T}{\partial z^2} - QT\right\} + Br\left[\frac{\partial U}{\partial z}\right]^2 \tag{11}$$

$$\frac{\partial C}{\partial t} - S\frac{\partial C}{\partial z} = \frac{1}{Sc}\frac{\partial^2 C}{\partial z^2} + Sr\frac{\partial^2 T}{\partial z^2} - KrC \tag{12}$$

where $A_1 = (1-\emptyset)^{2.5}$, $A_2 = \frac{K_{nf}}{K_f}, A_3 = 1 - \emptyset + \emptyset\left(\frac{p_s}{p_f}\right), A_4 = 1 - \emptyset + \emptyset(p\beta)/(p\beta)_f$

$A_5 = 1 - \emptyset + \emptyset\left(\rho C_p\right)/(\rho C_p)_f$

The relevant boundary conditions now become:

u(z, t) = 0, v(z, t) = 0, T(z, t)=0, C(z, t)=0 for $t \le 0$ $any\ z$

u(0, t)=1+$\frac{\varepsilon}{2}(e^{int} + e^{-int})$, $v(0,t) = 0, T(0,t) = 1, C(0,t) = 1$

$$u(\infty,t) \to 0, v(\infty,t) \to 0, T(\infty,t) \to 0, C(\infty,t) \to 0\ for\ t \ge 0 \tag{13}$$

Using eqn (9) the velocity characteristics U_0 is defined as:

$U_0 = \{g\beta_f(T_w - T_\infty)vf\}^{1/3}$

To obtain the desired solutions, we now simplify eqns (9-12) by putting the fluid velocity in the complex form as: $U(z,t) = u(z,t) + iv(z,t)$ and we get

$$A_3\left\{\frac{\partial U}{\partial t} - S\frac{\partial U}{\partial z} - iRU\right\} = \frac{1}{A_1}\frac{\partial^2 U}{\partial z^2} + A_4 T - \left(M + \frac{1}{K}\right)U \tag{14}$$

The associated boundary conditions in eqn (13) become:

U(z, t) = 0, T(z, t)=0, C(z, t)=0 for $t \le 0$ $any\ z$

U(0, t)=1+$\frac{\varepsilon}{2}(e^{int} + e^{-int}), T(0,t) = 1, C(0,t) = 1$

$$U(\infty,t) \to 0, v(\infty,t) \to 0, T(\infty,t) \to 0, C(\infty,t) \to 0\ for\ t \ge 0 \tag{15}$$

3. Method of Solutions

To find the analytical solutions of the above system of partial differential equations (11), (12) and (14) subject to the boundary conditions (15) in the neighbourhood of the plate, we assume that (see Ganepathy (1994))

$$U(z,t) = U_0(z,t) + \frac{\varepsilon}{2}\{e^{int}U_1\} \tag{16}$$

$$T(z,t) = T_0(z,t) + \frac{\varepsilon}{2}\{e^{int}T_1\} \tag{17}$$

$$C(z,t) = C_0(z,t) + \frac{\varepsilon}{2}\{e^{int}C_1\} \tag{18}$$

Due to the nonlinearity of this resultant governing equations, we further make the following assumptions:

$$\left.\begin{aligned} U_0(z,t) &= U_{00}(z,t) + Br[U_{01}(z,t)] \\ U_1(z,t) &= U_{10}(z,t) + Br[U_{11}(z,t)] \end{aligned}\right\} \tag{19}$$

$$\left.\begin{aligned} T_0(z,t) &= T_{00}(z,t) + Br[T_{01}(z,t)] \\ T_1(z,t) &= T_{10}(z,t) + Br[T_{11}(z,t)] \end{aligned}\right\} \tag{20}$$

$$\left.\begin{aligned} C_0(z,t) &= C_{00}(z,t) + Br[C_{01}(z,t)] \\ C_1(z,t) &= C_{10}(z,t) + Br[C_{11}(z,t)] \end{aligned}\right\} \tag{21}$$

Substituting eqns (19-21) into eqns (11), (12) and (14), and comparing the coefficients of Br^0 and Br^1, after involving the above equations (16-18) into eqns (9-12) and equating the harmonic and non-harmonic terms and neglecting the higher order terms of $O(\varepsilon^2)$, we obtain the following set of equations:

The zeroth order equations are:

Velocity equations

$$\frac{1}{A_1}\frac{\partial^2 U_{00}}{\partial z^2} + A_3 S\frac{\partial U_{00}}{\partial z} - \left(A_3 iR + M + \frac{1}{K}\right)U_{00} + A_4 T_{00} = 0 \tag{22}$$

$$\frac{1}{A_1}\frac{\partial^2 U_{01}}{\partial z^2} + A_3 S\frac{\partial U_{01}}{\partial z} - \left(A_3 iR + M + \frac{1}{K}\right)U_{01} + A_4 T_{01} = 0 \tag{23}$$

Temperature equations

$$A_2\frac{\partial^2 T_{00}}{\partial z^2} + A_5 SPr\frac{\partial T_{00}}{\partial z} - QT_{00} = 0 \tag{24}$$

$$A_2\frac{\partial^2 T_{01}}{\partial z^2} + A_5 SPr\frac{\partial T_{01}}{\partial z} - QT_{01} = -Pr\left[\frac{\partial U_{00}}{\partial z}\right]^2 \tag{25}$$

Concentration equations

$$\frac{\partial^2 C_{00}}{\partial z^2} + SSc\frac{\partial C_{00}}{\partial z} - ScKrC_{00} = -ScSr\frac{\partial^2 T_{00}}{\partial z^2} \tag{26}$$

$$\frac{\partial^2 C_{01}}{\partial z^2} + SSc\frac{\partial C_{01}}{\partial z} - ScKrC_{01} = -ScSr\frac{\partial^2 T_{01}}{\partial z^2} \tag{27}$$

The first order equations are

Velocity equations

$$\frac{1}{A_1}\frac{\partial^2 U_{10}}{\partial z^2} + A_3 S\frac{\partial U_{10}}{\partial z} - \left(A_3 iR + M + \frac{1}{K}\right)U_{10} + A_4 T_{10} = 0 \tag{28}$$

$$\frac{1}{A_1}\frac{\partial^2 U_{11}}{\partial z^2} + A_3 S\frac{\partial U_{11}}{\partial z} - \left(A_3 iR + M + \frac{1}{K}\right)U_{11} + A_4 T_{11} = 0 \tag{29}$$

Temperature equations

$$A_2\frac{\partial^2 T_{10}}{\partial z^2} + A_5 SPr\frac{\partial T_{10}}{\partial z} - QT_{10} = 0 \tag{30}$$

$$A_2\frac{\partial^2 T_{11}}{\partial z^2} + A_5 SPr\frac{\partial T_{11}}{\partial z} - QT_{11} = -Pr\left[\frac{\partial U_{10}}{\partial z}\right]^2 \tag{31}$$

Concentration equations

$$\frac{\partial^2 C_{10}}{\partial z^2} + SSc\frac{\partial C_{10}}{\partial z} - ScKrC_{10} = -ScSr\frac{\partial^2 T_{10}}{\partial z^2} \tag{32}$$

$$\frac{\partial^2 C_{11}}{\partial z^2} + SSc\frac{\partial C_{11}}{\partial z} - ScKrC_{11} = -ScSr\frac{\partial^2 T_{11}}{\partial z^2} \tag{33}$$

The corresponding boundary conditions can simply be written as:

$$\begin{gathered} U_{00} = U_{01} = U_{10} = U_{11} = 1, T_{00} = T_{01} = T_{10} = T_{11} = 1, C_{00} = C_{01} = C_{10} = C_{11} = 1 \; at \; z = 0 \\ U_{00} = U_{01} = U_{10} = U_{11} = 0, T_{00} = T_{01} = T_{10} = T_{11} = 0, C_{00} = C_{01} = C_{10} = C_{11} = 0 \; at \; z \to \infty \end{gathered} \tag{34}$$

Solving the above equations restricted to the boundary conditions (34), we obtain the expressions for velocity, temperature and concentration as:

$$T_{00} = e^{-c_2 z} \tag{35}$$

$$T_{01} = F_4 e^{-c_4 z} + F_5 e^{-2c_{18} z} + F_6 e^{-c_{18} - c_2 z} + F_7 e^{-2c_2 z} \tag{36}$$

$$T_{10} = e^{-c_6 z} \tag{37}$$

$$T_{11} = F_9 e^{-c_8 z} + F_{10} e^{-2c_{20} z} + F_{11} e^{-c_{20} - c_6 z} + F_{12} e^{-2c_6 z} \tag{38}$$

$$C_{00} = B_2 e^{-c_{10} z} + B_3 e^{-c_2 z} \tag{39}$$

$$C_{01} = B_5 e^{-c_{12} z} + B_6 e^{-c_4 z} + B_7 e^{-2c_{18} z} + B_8 e^{-c_{18} z - c_4 z} + B_9 e^{-2c_2 z} \tag{40}$$

$$C_{10} = B_9 e^{-c_{14} z} + B_{10} e^{-c_6 z} \tag{41}$$

$$C_{11} = B_{14} e^{-c_{16} z} + B_{15} e^{-c_8 z} + B_{16} e^{-2c_{20} z} + B_{17} e^{-c_{20} - c_6 z} + B_{18} e^{-2c_6 z} \tag{42}$$

$$U_{00} = D_2 e^{-c_{18} z} + D_3 e^{-c_2 z} \tag{43}$$

$$U_{01} = D_5 e^{-c_{20} z} + D_6 e^{-c_4 z} + D_7 e^{-2c_{18} z} + D_8 e^{-c_{18} z - c_2 z} + D_9 e^{-2c_2 z} \tag{44}$$

$$U_{10} = D_9 e^{-c_{20} z} + D_{10} e^{-c_6 z} \tag{45}$$

$$U_{11} = D_{13} e^{-c_{22} z} + D_{14} e^{-c_8 z} + D_{15} e^{-2c_{20} z} + D_{16} e^{-c_{20} z - c_8 z} + D_{17} e^{-2c_6 z} \tag{46}$$

Recall that,

$$U(z,t) = U_0 + \frac{\varepsilon}{2}\{e^{int} U_1\} \tag{47}$$

$$T(z,t) = T_0 + \frac{\varepsilon}{2}\{e^{int} T_1\} \tag{48}$$

$$C(z,t) = C_0 + \frac{\varepsilon}{2}\{e^{int} C_1\} \tag{49}$$

The physical quantities of engineering interest are also calculated such as skin friction, Nusselt number and Sherwood number coefficients, which have been derived as:

$$\left.\frac{dU}{dz}\right|_{z=0} = -c_{18}D_2 - c_2D_3 + Br(-c_{20}D_5 - c_4D_6 - 2c_{18}D_7 - (c_{18} + c_2)D_8 - 2c_2D_9) + \frac{\varepsilon}{2}[-c_{20}D_{10} - c_6D_{11} + Br(-c_{22}D_{13} - c_8D_{14} - 2c_{20}D_{15} - (c_{20} + c_6)D_{16} - 2c_6D_{17})]e^{int} \tag{50}$$

$$\left.\frac{dT}{dz}\right|_{z=0} = -c_2 + Br(-c_4F_4 - 2c_{18}F_5 - (c_{18} + c_2)F_6 + -2c_2F_7) + \frac{\varepsilon}{2}[-c_6 + Br(-c_8F_9 - 2c_{20}F_{10} - (c_{20} + c_6)F_{11} + -2c_6F_{12})]e^{int} \tag{51}$$

$$\left.\frac{dC}{dz}\right|_{z=0} = -c_{10}B_2 - c_2B_3 + Br(-c_{12}B_5 - c_4B_6 - 2c_{18}B_7 - (c_{18} + c_2)B_8 - c_4B_9) + \frac{\varepsilon}{2}[-c_{14}B_9 - c_6B_{10} + Br(-c_{16}B_{14} - c_8B_{15} - 2c_{20}B_{16} - (c_{20} + c_6)B_{17} - 2c_6B_{18})]e^{int} \tag{52}$$

The expressions for all constants are provided in the appendix section.

4. Results and Discussion

In this section, we present the results and discussion of the investigation of the impacts of viscous dissipation and permeability on MHD oscillatory heat and mass flow across a porous channel affected by thermal diffusion, chemical reaction and heat absorption. In order to get physical insight into the problem, we have carried out numerical evaluation for non-dimensional velocity, temperature and species concentration, skin-friction, and Nusselt number by assigning some specific values to the embedded parameters dictating the flow for basically two different types of water based nanofluids. For this purpose, Figures 3-11 have been plotted and discussed. Table1 shows the thermo physical properties of water and the Nano elements Cu, Ai_2O_3 and TiO_2. To ascertain the validity and correctness of this present investigation, the graphs for temperature and velocity profiles as shown in Figure 2a and b for Narayana and Venkateswarlu (2016) and the current study for limiting case when $Br \rightarrow 0$ for fixed values of ε =0.01; R=0.02 n=10.0; t=0.1; M=0.5, K=S=Kr=1; Q=10.0: $\emptyset = 0.15$.

Table 1: Thermo-physical properties

Physical properties	Water	Copper (Cu)	Aluminium Oxide (Al_2O_2)	Titanium oxide (TiO_2)
C_p	4179	385	765	686.2
ρ	997.1	8933	3970	4250
K	0.613	400	40	8.9538
$\beta \times 10^{-5}$	21	1.67	0.85	0.9

The comparison demonstrates an excellent relationship. Figures 3 and 4 present the effects of the viscous dissipation parameter Br on the temperature and velocity gradients respectively. With an increase in Br, the temperature of the fluid increases. Equally, an increase in Br results to an increase in the fluid velocity. Rising Brickman numbers mean correspondingly higher degrees of convective heating at the lower channel wall and consequently lead to high temperature and velocity at the lower plate. Makinde and Aziz (2011) reported that, increasing the local Brickman numbers leads to the stronger convective heating at the lower channel wall which results in higher surface temperatures causing the thermal effect to penetrate deeper into the quiescent fluid, consequently making the fluid motion to escalate. The deviations of temperature profiles for different values of heat sink parameter Q is sketched in Figure 5. It is clear that, there is a decrease in the temperature with increase of Q. This is due to the fact that when heat is absorbed, the buoyancy forces decrease which retard the flow rate and thereby give rise to a decrease in the temperature profile. The variations of Darcy porous parameter on the velocity gradient is illustrated in Figure 6. It is depicted from this figure that the action of the Darcy porosity parameter on the velocity nanoparticles gradient. It is perceived from this figure that the velocity fluid accelerates as the porosity parameter is increased. We observe that, with the growth in permeability of the porous medium, the drag force weakens; because of this, velocity gradient of the fluid blows up. Moreover, this makes sense because when a lot of fluid is moved, more viscous energy is made. This causes the fluid boundary wall and thickness to grow, which speeds up the movement of the fluid. Figure 7 shows the influence of magnetic field parameter M on the velocity Nanofluid profiles in the boundary layer. Application of magnetic field to an electrically conducting fluid gives rise to a resistive type force called the Lorentz force. This force has the tendency to slow down the motion of the fluid in the boundary layer.

Thus, the presence of the magnetic field parameter decreases the momentum boundary layers' thickness. Figure 8 shows the effect of chemical reaction (Kr) on concentration profile. Its observed that increase in chemical reaction parameter decreases the concentration profile. The rationale is that as chemical reactions increases, the quantity of solute molecules undergoing them grows, this causes concentration to drop, which in turn reduces the likely-hood of destructive chemical reaction. In other words, the concentration asymptotically decreases from the maximum value 1 to 0 as z →∞. This shows that the concentration field is greatest near the plate surface and least in the outer flow region. The same figure further indicates that there is a steady fall in species concentration due to the effect of chemical reaction. This means that the consumption of chemical species leads to fall in the species concentration field. This clearly agrees with the physical laws. Figure 9 demonstrates how the species concentration rises along with the number of Sorets. A rise in the Soret effect, by definition, indicates an increase in molar mass diffusivity. An increase in the increase in concentration is due to molecule mass diffusivity. This shows that the species concentration in the fluid tends to rise as the Soret number rises. The deviations of magnetic number versus suction/injection parameters on the skin friction is displayed in Figure 10. It is evident that increasing the magnetic and suction/injection effects strengthens the skin friction and this effect is higher in the case of Cu-water nano element than Ai_2O_3 and TiO_2 nano elements. The impact of Br on the shear stress against suction/injection is exhibited in Figure 11. The exhibition explains that higher Br encourages the skin friction particularly at the heated plate. The coefficient of Nusselt number is plotted against Q for different values of Br in Figure 12. It is obvious that the rates of heat transfer increase with rising values of Br. It is also observed that Cu -water nanofluid has the highest Nusselt number.

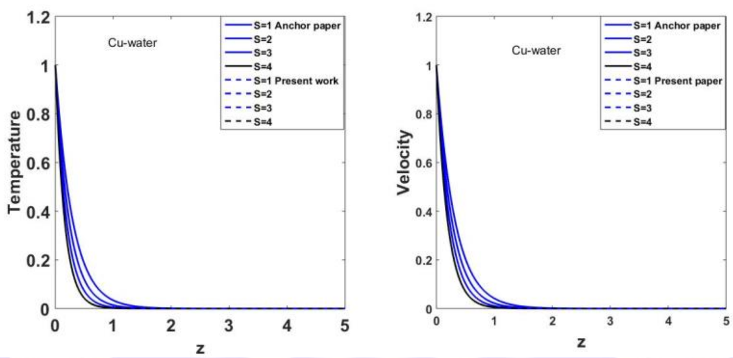

Figure 2: Comparison of Narayana and Venkateswarlu 2016 with the present work for (a) temperature and (b) velocity gradient

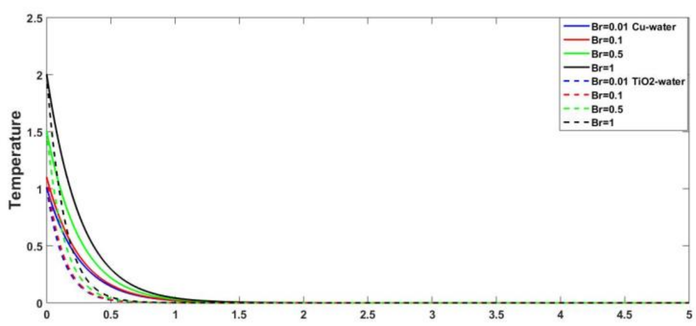

Figure 3: Application of Br on temperature distribution

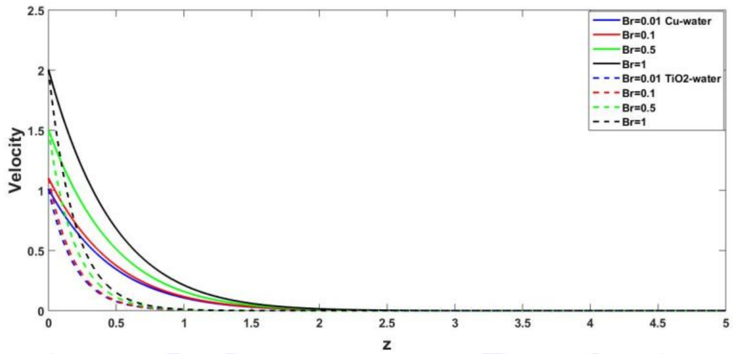

Figure 4: Application of Br on Velocity distribution

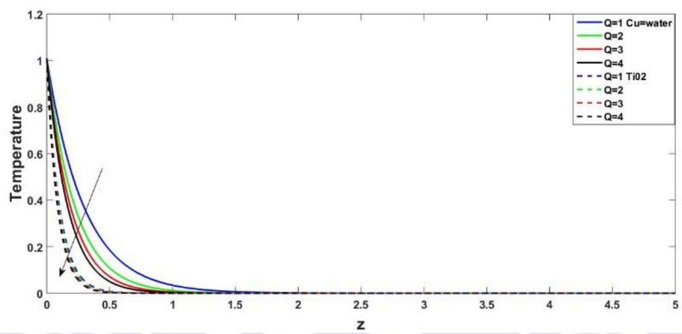

Figure 5: Application of Q on temperature distribution

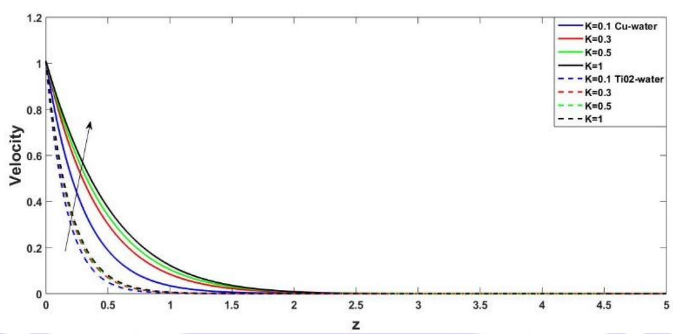

Figure 6: Application of K on velocity distribution

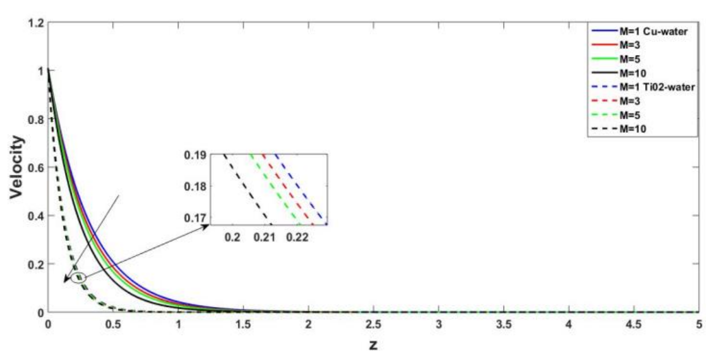

Figure 7: Application of M on velocity distribution

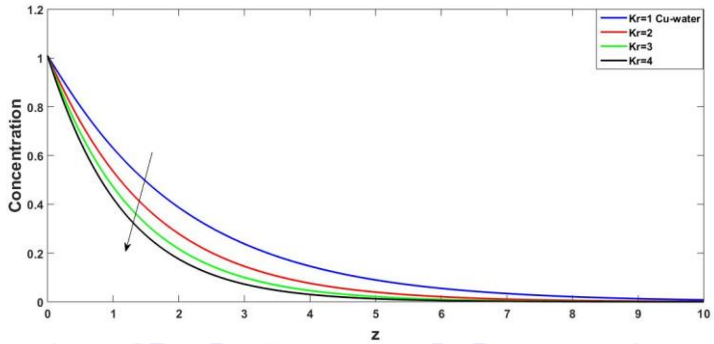

Figure 8: Application of Kr on concentration distribution

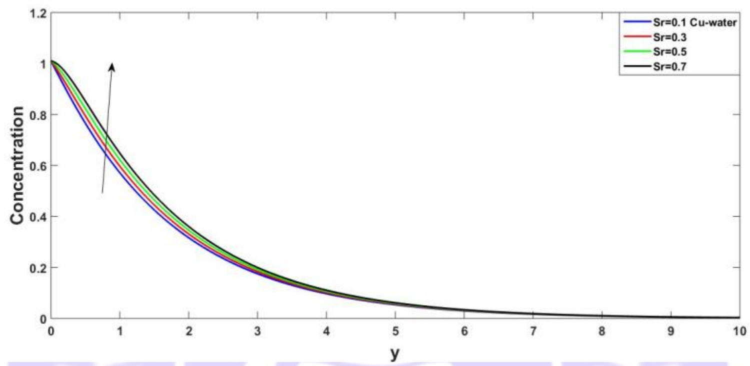

Figure 9: Application of Sr on concentration distribution

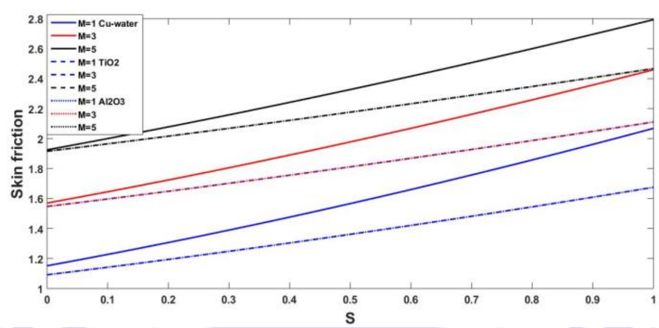

Figure 10: Application of M versus S on skin friction

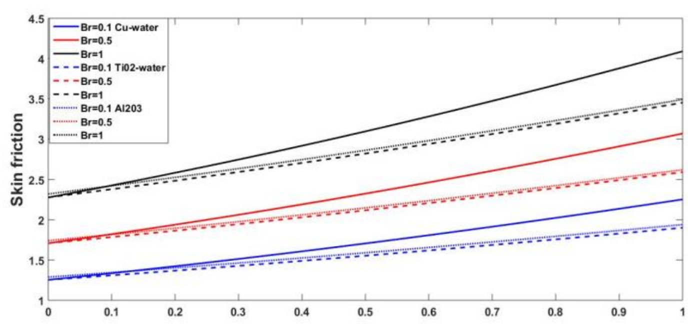

Figure 11: Application of Br against S on Skin friction

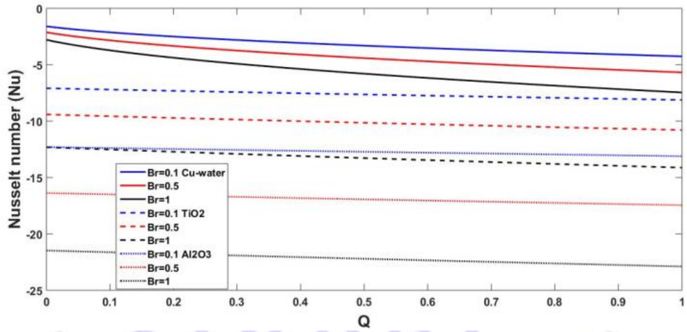

Figure 12: Application of Br against Q on Nusselt number

5. Conclusion

The effect of Brickman number representing the viscous dissipation on heat and mass transfer on MHD oscillatory nanofluid flow in a permeable plate equipped with porous material was considered and researched. The nanofluid velocity, temperature and concentration profiles have been calculated for pertinent controlling parameters on the flow configuration. The physical components of engineering interest have also been computed such as nanofluid skin friction, Nusselt number and Sherwood number. We hope that the findings of this investigation may be useful in catalysis, biomedicine, magnetic resonance imaging, data storage and environmental remediation. Hence, the subject of nanofluids is of great interest worldwide for basic and applied research. The summary of the noteworthy findings is given below:

i. It is concluded that increasing the Brickman number leads to an increase in fluid nanoparticle temperature and velocity respectively.

ii. The copper nanoparticles proved to have the maximum cooling recital for this vertical porous plate problem where Alumina nanoparticles have the lowest. This is due to the high thermal conductivity of Cu and low thermal conductivity of Al_2O_3 and TiO_2

iii. The velocity profile decreases with an increase in nanoparticle magnetic parameter, while the opposite is true when the Darcy porous parameter is increased.

iv. Due to chemical reaction, the concentration of the fluid decreases. This is because the consumption of chemical species leads to a fall in the species concentration field. This remarkable feature of the concentration profiles in our investigation is due to the presence of Soret number and nanoparticles in the flow field.

v. It has been shown that mixing nanoparticles in a liquid (nanofluid) has a dramatic effect on the liquid thermophysical properties such as thermal conductivity.

Acknowledgement

The authors are immensely grateful to Tertiary Education Trust Fund (TETFUND, Nigeria) for funding support to Federal University Gusau under the Institutional Based Research (IBR) scheme (Project No: TETF/DRandD/UNI/GUSAU/IBR/2024/VOL.I).

Conflict of Interest

The authors have declared no conflict of interest.

References

Abbas, M. A., Ahmed, B., Li, C., Rehman, S. U., Saleem, M. and Khudair, W. S. (2022). Analysis of entropy generation on magnetohydrodynamic flow with mixed convection through porous media, *Energies,* 15 (3), 1206, https://doi.org/10.3390/en15031206.

Ajibade A. O., Gambo J. J. and Jha B. K. (2023). Effects of viscous and Darcy dissipation on fully developed natural convection flow in a composite channel partially filled with porous material: Homotopy perturbation method (HPM), Journal of Applied Mathematics and Mechanics, 103(6), https//doi.org/10.1002/zamm.202100583

Ajibade, A.O. and Umar, A.M. (2016). Effect of chemical reaction and radiation absorption on the unsteady MHD free convection Couette flow in a vertical channel filled with porous materials. *Afrika Matematika*, 27, 201–213.

Alam Md. Shariful (2016). Effect of Thermophoresis on MHD Free Convective Heat and Mass Transfer Flow along an Inclined Stretching Sheet under the Influence of Dufour-Soret Effects with Variable Wall Temperature, *Thammasat International Journal of Science and Technology,* 21(3), pp 48-58.

Alam N., Poddar S., Karim M. E, Hasan M. S. and Lorenzini G. (2021). Transient MHD radiative fluid flow over an inclined porous plate with thermal and mass diffusion: an EFDM numerical approach. *International Information of Engineering and Technological Associations,* **8**(5), pp. 739-749.

Alvarez, M., Colmenares, E. and Sequeira, F. A. (2022). Analysis of a semi-augmented mixed finite element method for double-diffusive natural convection in porous media, *Computational Mathematics and Applications,* 114, pp. 112–131, https://doi.org/10.1016/j.camwa.2022.03.032.

Bafakeeh O. T., Raza A., Khan U. S., Khan M. I., Nasr A., Khedher N.B. and Tag-Eldin E.M. (2022). Physical interpretation of Nanofluid (Copper Oxide and Silver) with slip and mixed convection effects: Application of fractional derivatives; *Applied Sciences*, 12 (21), 10860.

Baoku, I. and Fadare, S.A. (2018). Thermo-diffusion and diffusion -thermo effects on mixed convection hydromagnetic flow in a third-grade fluid over a stretching surface in a Darcy forchheimer porous medium. *FUDMA Journal of Sciences*, 2(1), pp. 23-42.

Bordoloi R, Chamuah K., and Ahmed N. (2023). Free Convective MHD Radiative Flow Past a Porous Vertical Plate in a Porous Medium with Chemical Reaction, *Biointerface Research in Applied Chemistry*, 13 (3), 1-15.

Bordoloi, R. Ahmed, N. Kakati, L. (2021). Dufour effect on three-dimensional flow past a porous vertical plate in a porous medium with periodic suction and permeability, *Journal of Heat and Mass Transfer*, 24, 283-308, http://dx.doi.org/10.17654/0973576321005.

Casson, N. (1959). Flow equation for pigment oil suspensions of the printing ink type. Rheology of disperse systems, 84(2), Choi, S.U., Eastman, J. A. Enhancing thermal conductivity of fluids with nanoparticles. No. ANL/MSD/CP-84938: CONF-951135-29.

Chitra M. and Suhasini M. (2018). Effect of unsteady oscillatory MHD flow through a porous medium in porous vertical channel with chemical reaction and concentration, *National Conference on Mathematical Techniques and its Applications*, 012039, doi :10.1088/1742-6596/1000/1/012039

Choi, S.U. and Eastman, J.A. (1995). Enhancing thermal conductivity of fluids with nanoparticles. (No. ANL/MSD/CP-84938: CONF-951135-29.

Choudhury M and Hazarika G. C. (2012). The Effects of Variable Viscosity and Thermal Conductivity on MHD Oscillatory Free Convective Flow past a Vertical Plate in Slip Flow Regime with Variable Suction and Periodic Plate Temperature, *Journal of Applied Fluid Mechanics,* 6(2), pp. 277-283.

Falade, J. A., Ukaegbu, J., Egere, A. C., and Adesanya, S., (2017). MHD Oscillatory Flow Through a Porous Channel Saturated with Porous Medium, Alexandria Eng. J., 56(1), pp. 147–152.

Gbadeyan, J.A., Titiloye, E.O., and Adeosun, A.T. (2020). Effect of variable thermal conductivity and viscosity on

Casson nanoflui9d flow with convective heating and velocity slip. *Heliyon,* 6(1), e03076.

Gireesha B. J. and S. Sindhu, (2020). MHD natural convection flow of casson fluid in an annular microchannel containing porous medium with heat generation/absorption. *Nonlinear Engineering*, **9**, pp. 23-232.

Hamza, M. M., Shuaibu A. and Ahmad, S. K. (2022). Unsteady MHD free convection flow of an exothermic fluid in a convectively heated vertical channel filled with porous medium, *Scientific Reports*,**12**, 11989.

Hamza, M.M. Usman, H. Mustafa A. and Isah B.Y. (2011). Chemical Reaction and Slip Condition Effects on MHD Oscillatory Flow Through a Porous Medium, *Research Journal of Mathematic and Statistics*, 3(4), pp. 130-135

Ibrahim, F., Elaiw, A. and Bakr, A. (2008). Effect of the chemical reaction and radiation absorption on the unsteady MHD free convection flow past a semi infinite vertical permeable moving plate with heat source and suction. *Communication in Nonlinear Scienc and Numerical Simulation*, 13, 1056–1066.

Kadeethum, T., Ballarin, F., Choi, Y., O'Malley, D., Yoon, H and Bouklas, N. (2022). Non-intrusive reduced order modeling of natural convection in porous media using convolutional autoencoders: comparison with linear subspace techniques, *Advances in Water Resources,* 160, 104098.

Kesavaiah, D. C., Satyanarayana, P. and Venkataramana, S. (2011). Effects of the chemical reaction and radiation absorption on an unsteady MHD convective heat and mass transfer flow past a semi-infinite vertical permeable moving plate embedded in a porous medium with heat source and suction. *International Journal Applied Mathematics and Mechanics*,7, 52–69.

Khalil, W. H., Azzawi, I.D.J. and Damook, A.A. (2022). The optimisation of MHD free convection inside porous trapezoidal cavity with the wavy bottom wall using response surface method, *International Communications in Heat and Mass Transfer,* 134, 106035, https://doi.org/10.1016/j.icheatmasstransfer.2022.106035.

Khedher, N. B., Ullah, Z., Mahrous, Y. M., Dhahbi, S., Ahmad, S., Abu-Zinadah, H., and Faqihi, A. A. (2024). Viscous dissipation effect on amplitude and oscillating frequency of heat transfer and electromagnetic waves of magnetic driven fluid flow along the horizontal circular cylinder. *Case Studies in Thermal Engineering*, 55. https://doi.org/10.1016/j.csite.2024.104142

Mabood, F., and Usman, H. (2019). Multiple slip effects on MHD thermo-solutal flow in porous media saturated by nanofluid. *Mathematical modelling of engineering problems,* 6(4), 502-510.

Mahmoudi Y, Hooman K and Vafai K, (2020). Convective Heat Transfer in Porous Media (New York, USA: Taylor and Francis Group, LLC CRC Press)

Mehryan, M., Moradi S.A., Kashkooli, F., Soltani, M. and Raahemifar, K. (2016). Fluid flow and heat transfer analysis of a nanofluid containing motile gyrotactic micro-organisms passing a nonlinear stretching vertical sheet in the presence of a non-uniform magnetic field; numerical approach. *PLos One*, 11(6), e0157598.

Mukwabi, L. K., Kimathi, M. and Muli C. (2023). Effects of Brownian motion and thermophoresis variation on mhd nanofluid flow in a concentrated parabolic thermal solar collector, *International Journal of Novel Research in Physics Chemistry and Mathematics*, 10(1), pp. 25-37.

Mustafa, M., Hina S., Hayat T. and Alsaedi A. (2012). Influence of wall properties on the peristaltic flow of a nanofluid: Analytic and numerical solutions. *International Journal of Heat and Mass Transfer,* 55(17), 4871–4877.

Muthucumaraswamy, R. (2002). Effects of a chemical reaction on a moving isothermal vertical surface with suction. *Acta Mechanica*, 155, 65–70.

Narayana P.V. S. and Venkateswarlu B. (2016). Heat and mass transfer on mhd nanofluid flow past a vertical porous plate in a rotating system, *Frontiers in Heat and Mass Transfer,* 7(8), DOI: 10.5098/hmt.7.8

Omar T. B., Raghunath K., Ali F., Khalid M., Tag-ElDin E. M., Oreijah M., Guedri K., Khedher N. B. and Khan M. I. (2022). Hall Current and Soret Effects on Unsteady MHD Rotating Flow of Second-Grade Fluid through Porous Media under the Influences of Thermal Radiation and Chemical Reactions, *Catalysts,* 12, 1233. https://doi.org/10.3390/ catal12101233

Prasad, P.D., Kumar, R.K., and Varma, S.V.K. (2018) heat and mass transfer analysis for the MHD flow of nanofluid with radiation absorption. *Ain Shams Engineering Journal*, 9(4), 801-813.

Raghunath, K. and Obulesu, M. (2022). Unsteady MHD oscillatory Casson fluid flow past an inclined vertical porous plate in the presence of chemical reaction with heat absorption and Soret effects. *Heat Transfer*, 51, 733–752.

Raghunath, K., Nagesh, G., Reddy, V.R.C. and Obulesu, M. (2021). Unsteady MHD fluid flow past an inclined vertical porous plate in the presence of chemical reaction with aligned magnetic field, radiation, and Soret effects. *Heat Transfer*,51,2742–2760.

Raghunath, K., Obulesu, M., Sujatha, S. and Venkateswaraju, K. (2022). Investigation of MHD Casson fluid flow past a vertical porous plate under the influence of thermal diffusion and chemical reaction. *Heat Transfer*, 51, 377–394.

Ramaiah, P., Vijaya S., Kumar V. K., Prasad R. K. and Balamurugan k. S. (2016). Chemical reaction and radiation absorbtion effects on MHD convective heat and mass transfer flow of a viscoelastic fluid past an oscillating porous plate with heat generation/absorption, *International Journal of Chemical Sciences,* 14(2), pp. 570-584

Reddy, V. R., Raghunath, K. and Obulesu, M. (2022). Characteristics of MHD Casson fluid past an inclined vertical porous plate. *Material Today for Proceses.*, 49, 2136–2142.

Salah F., Sidahmed A. O. M. and Viswanathan K. K. (2023). Chemical MHD Hiemenz flow over a nonlinear stretching sheet and Brownian motion effects of nanoparticles through a porous medium with radiation effect, *Mathematical Computer and Modeling of Fluid Flow and Heat Transfer*, 28(1), 21, DOI: 10.3390/mca28010021

Saleem, S., Nazeer, M., Radwan, N., and Abutuqayqah, H. (2024). Significance of hafnium nanoparticles in hydromagnetic non-Newtonian fluid-particle suspension model through divergent channel with uniform heat source: thermal analysis. *Zeitschrift für Naturforschung A*, (0). https://doi.org/10.1515/zna-2023-0336

Salleh, M. Z., Nazar, R., and Pop, I. (2010). Mixed convection boundary layer flow over a horizontal circular cylinder with Newtonian heating. *Heat and mass transfer*, 46, 1411-1418.

Sharma T., Sharma P. and Kumar N. (2022). Study of dissipative MHD oscillatory unsteady free convective flow in a vertical channel occupied with the porous material in the presence of heat source effect and thermal radiation, *International Symposium on Fluids and Thermal Engineering*, 012012. doi:10.1088/1742-6596/2178/1/012012.

Usman and Sanusi (2023). Heat and mass transfer analysis for the mhd flow of Casson nanofluid in the presence of thermal radiation, *FUDMA Journal of Sciences,* 7(2), pp 188 – 198.

Appendix

$c_1 = c_3 = c_5 = c_7 = \frac{-A_5SPr+\sqrt{(A_5SPr)^2+4A_2Q}}{2A_2}$, $c_2 = c_4 = c_6 = c_8 = \frac{A_5SPr+\sqrt{(A_5SPr)^2+4A_2Q}}{2A_2}$,
$c_9 = c_{11} = c_{13} = c_{15} = \frac{-SSc+\sqrt{(SSc)^2+4ScKr}}{2}$, $c_{10} = c_{12} = c_{14} = c_{16} = \frac{SSc+\sqrt{(SSc)^2+4ScKr}}{2}$,
$c_{17} = c_{19} = c_{21} = c_{23} = \frac{-A_1A_3S+\sqrt{(A_1A_3S)^2+4A_1w_2}}{2}$, $c_{18} = c_{20} = c_{22} = c_{24} = \frac{A_1A_3S+\sqrt{(A_1A_3S)^2+4A_1w_2}}{2}$,
$w_2 = A_3iR + M + \frac{1}{K}$, $F_5 = \frac{-Prc_{18}^2D_2^2}{4A_2c_{18}^2-2A_5SPrc_{18}-Q}$, $F_6 = \frac{-2Prc_2c_{18}D_2D_3}{A_2(-c_{18}-c_2)^2-A_5SPr(-c_{18}-c_2)-Q}$, $F_7 = \frac{-Prc_2^2D_3^2}{4A_2c_2^2-2A_5SPrc_2-Q}$, $F_4 = 1 - F_5 - F_6 - F_7$, $F_{10} = \frac{-Prc_{20}^2D_{10}^2}{4A_2c_{20}^2-2A_5SPrc_{20}-Q}$, $F_{11} = \frac{-2Prc_6c_{20}D_{10}D_{11}}{A_2(-c_{20}-c_6)^2-A_5SPr(-c_{20}-c_6)-Q}$, $F_{12} = \frac{-Prc_6^2D_{11}^2}{4A_2c_6^2-2A_5SPrc_6-Q}$, $F_9 = 1 - F_{10} - F_{11} - F_{12}$, $B_3 = \frac{-ScSrc_2^2}{4c_2^2-SScc_2-ScKr}$, $B_2 = 1 - B_3$, $B_6 = \frac{-ScSrc_4^2F_4}{c_4^2-SScc_4-ScKr}$, $B_7 = \frac{-4ScSrc_{18}^2F_5}{4c_{18}^2-2SScc_{18}-ScKr}$, $B_8 = \frac{-ScSr(-c_{18}-c_2)F_6}{(-c_{18}-c_2)^2-SSc(-c_{18}-c_2)-ScKr}$, $B_9 = \frac{-4ScSrc_2^2F_7}{4c_2^2-2SScc_2-ScKr}$, $B_5 = 1 - B_6 - B_7 - B_8 - B_9$,
$B_{11} = 1 - B_{12}$, $B_{15} = \frac{-ScSrc_8^2F_9}{c_8^2-SScc_8-ScKr}$, $B_{16} = \frac{-4ScSrc_{20}^2F_{10}}{4c_{20}^2-2SScc_{20}-ScKr}$, $B_{17} = \frac{-4ScSr(-c_{20}-c_6)^2F_{11}}{4(-c_{20}-c_6)^2-SSc(-c_{20}-c_6)-ScKr}$, $B_{18} = \frac{-4ScSrc_6^2F_{12}}{4c_6^2-2SScc_6-ScKr}$, $B_{14} = 1 - B_{15} - B_{16} - B_{17} - B_{18}$, $D_3 = \frac{-A_4}{\frac{c_2^2}{A_1}-A_3Sc_2-w_2}$ $D_2 = 1 - D_3$, $D_6 = \frac{-A_4F_4}{\frac{c_4^2}{A_1}-A_3Sc_4-w_2}$, $D_7 = \frac{-A_4F_5}{\frac{c_{18}^2}{A_1}-A_3Sc_{18}-w_2}$, $D_8 = \frac{-A_4F_6}{\frac{(-c_{18}-c_2)^2}{A_1}-A_3S(-c_{18}-c_2)-w_2}$, $D_9 = \frac{-A_4F_7}{\frac{c_2^2}{A_1}-2A_3Sc_2-w_2}$, $D_5 = 1 - D_6 - D_7 - D_8 - D_9$,
$D_{10} = \frac{-A_4}{\frac{c_6^2}{A_1}-A_3Sc_6-w_2}$, $D_9 = 1 - D_{10}$, $D_{13} = \frac{-A_4}{4\frac{c_6^2}{A_1}-2A_3Sc_6-w_2}$, $D_{12} = 1 - D_{13}$,
$D_{15} = \frac{-A_4F_9}{\frac{c_8^2}{A_1}-A_3Sc_8-w_2}$, $D_{16} = \frac{-A_4F_{10}}{\frac{4c_{20}}{A_1}-2A_3Sc_{20}-w_2}$, $D_{17} = \frac{-A_4F_{11}}{\frac{(-c_{20}-c_6)^2}{A_1}-A_3S(-c_{20}-c_6)-w_2}$, $D_{18} = \frac{-A_4F_{12}}{\frac{4c_6^2}{A_1}-2A_3Sc_6-w_2}$, $D_{14} = 1 - D_{15} - D_{16} - D_{17} - D_{18}$,

Nomenclature

B_0	constant applied magnetic field
τ	skin friction coefficient
C_p	specific heat at constant pressure
C_∞	concentration of the solute far away from the plate
D_m	molecular diffusivity
E	applied electric field
g	acceleration due to gravity
K	permeability parameter
k	permeability of porous medium
$k*$	mean absorption coefficient
M	dimensionless magnetic field parameter
Nu	Nusselt number
Pr	Prandtl number
Br	Brickman number
Q	dimensional heat sink parameter
R	dimensional rotational parameter
Kr	chemical reaction parameter
S	suction parameter
Sc	Schmidt number
Sr	Soret number
Sh	Sherwood number
w	condition at the wall

T local Temperature of the Nano fluid
T_w wall temperature of the fluid
T_∞ temperature of the ambient Nano fluid
U_0 characteristic velocity
(u,v,w) velocity components along x and y axes

Greek Symbols
α thermal diffusivity
α_f thermal diffusivity of the fluid
α_{nf} thermal diffusivity of the nanofluid
β thermal expansion coefficient
β_f coefficient of thermal expansion of the fluid
β_s coefficient of thermal expansion of the solid
$(\rho C_p)_{nf}$ heat capacitance of the nanofluid
$\sigma *$ Stefan-Boltzmann constant parameter
σ electrical conductivity of the fluid
ρ_f density of the fluid friction
ρ_{nf} density of the nanofluid
ρ_s density of the solid friction
ν_f kinematic viscosity of the fluid
ν kinematic viscosity
μ_{nf} viscosity of the nanofluid
μ dynamic viscosity
ε small constant quantity
U complex velocity
T non-dimensional Temperature
C non-dimensional Concentration

Subscript
f fluid
s solid
n_f Nano fluid
∞ Condition at free stream